Applied Catalysis B: Environmental 132–133 (2013) 519–526

Contents lists available at SciVerse ScienceDirect

Applied Catalysis B: Environmental

journal homepage: www.elsevier.com/locate/apcatb

Review

Optimization of imazalil removal in the system UV/TiO_2/$K_2S_2O_8$ using a response surface methodology (RSM)

R. Hazime[a,c,*], Q.H. Nguyen[a,b], C. Ferronato[a], T.K.X. Huynh[b], F. Jaber[c], J.-M. Chovelon[a]

[a] Université de Lyon, Université Lyon 1, CNRS, UMR 5256, IRCELYON, Institut de recherches sur la catalyse et l'environnement de Lyon, 2 avenue Albert Einstein, F-69626 Villeurbanne, France

[b] Université Nationale du Vietnam à Ho Chi Minh ville, Département de Chimie Inorganique et Appliquée, Ecole des Sciences Naturelles, 227 Nguyen Van Cu, HCM ville, Vietnam

[c] Conseil National de la Recherche Scientifique, Commission Libanaise de l'Energie Atomique, Laboratoire d'Analyse de Pesticides et de Polluants Organiques, B. P. 11-8281, Riad El Solh, 1107 2260 Beyrouth, Liban

ARTICLE INFO

Article history:
Received 18 July 2012
Received in revised form
16 December 2012
Accepted 18 December 2012
Available online 24 December 2012

Keywords:
Imazalil degradation
UV/TiO_2/$K_2S_2O_8$
CCD
Experimental design
Persulfate

ABSTRACT

The optimization of the photocatalytic degradation of a carcinogen pesticide, imazalil, was carried out in an aqueous solution using TiO_2 as photocatalyst under UV irradiation in the presence of persulfate. Persulfate plays a double role; an electron scavenger and it promotes the formation of sulfate radicals which allow accelerating the removal of imazalil.

For the optimization, experimental design was used based on the surface response methodology; it was applied to assess the individual and interaction effects of several operating parameters (pH, TiO_2 concentration, pesticide concentration and persulfate concentration) on the treatment efficiency (90% of pesticide removal time).

Based on the experimental design data, a semi-empirical expression was obtained, permitting to predict and to optimize the pesticide removal time. This model was very consistent with experimental results (correlation factor: 99.15%). The strongest interactions between the parameters assessed were pH/[$K_2S_2O_8$] and [Imazalil]/[$K_2S_2O_8$]. Optimal experimental conditions found for imazalil (25 mg L^{-1}) removal were acidic pH 3–4, persulfate concentration (≈2.5 g L^{-1}) and TiO_2 loading (2.5 g L^{-1}). By using *tert*-butanol as hydroxyl radical scavenger, it was found that sulfate radicals were predominant at acidic pH and as the pH increases the hydroxyl radicals are more and more produced.

The experimental design allows obtaining the maximum of efficiency with the minimum amount of persulfate.

This work demonstrates well the utility and benefits of the experimental design approach for screening and modeling the reaction parameters.

Furthermore, it contributes significantly to the improvement and better understanding of photocatalytic processes using oxidants.

Contents

* Corresponding author. Tel.: +33 4 72 44 84 05; fax: +33 4 72 44 81 14.
E-mail addresses: roumaysa_hazimeh@live.com (R. Hazime), nqhuykhtn@gmail.com (Q.H. Nguyen), corinne.ferronato@ircelyon.univ-lyon1.fr (C. Ferronato), htkxuan@hcmus.edu.vn (T.K.X. Huynh), fjaber@cnrs.edu.lb (F. Jaber), jean-marc.chovelon@ircelyon.univ-lyon1.fr (J.-M. Chovelon).

0926-3373/$ – see front matter © 2012 Elsevier B.V. All rights reserved.
http://dx.doi.org/10.1016/j.apcatb.2012.12.021

1. Introduction

Advanced oxidation processes (AOP) usually coupled to light irradiation are more and more employed to the remediation of water pollutants [1]. AOPs including photocatalytic systems are based on the generation of hydroxyl radicals, which are highly reactive and nonselective oxidants toward organic compounds. As broadly accepted, photogenerated valence holes are formed when TiO_2 particles are irradiated by UV light, which leads to oxidation of OH^- or H_2O by holes resulting in hydroxyl radicals that are capable of destroying most organic species [2]. Oxygen acts efficiently as an electron trap, preventing the recombination of photogenerated electrons and holes. When oxygen is limited, the rapid recombination of electrons and holes in TiO_2 would markedly reduce its photocatalytic action [3]. Instead of oxygen, inorganic oxidants such as $S_2O_8^{2-}$, IO_4^-, BrO_3^-, ClO_3^- and H_2O_2 can be used [4–7]. These oxidants improve the performance of UV/TiO_2 by reducing the probability of recombination of the photogenerated electrons and holes, thus availing more holes for oxidative degradation of organic contaminants and by forming other reactive radicals ($SO_4^{\bullet-}$, $BrO^\bullet$, $BrO_2^\bullet$, $IO_3^\bullet$).

Persulfate is the newest oxidant that is being used for *in situ* chemical oxidation in the remediation of soil and groundwater [8]. It gives sulfate anions as end-product which are practically inert and not considered to be a pollutant [9].

Several authors have studied its effect on accelerating the degradation of organic compounds in UV/TiO_2. Selvam et al. [4] have shown that persulfate (0.1 M) is able to accelerate the degradation of 4– fluorophenol at acidic pH (pH 4) and alkaline pH (pH 9) and they found that the degradation is slightly more efficient in acidic medium. Syoufian and Nakashima [5] have used different concentrations of peroxydisulfate (0–20 mM) for the degradation of methylene blue and also concluded that this oxidant accelerates noticeably the degradation. Kashif and Ouyang [6] have compared different oxidants including persulfate, hydrogen peroxide and bromate (10 mM) at pH 5 (optimal value) for the degradation of phenol and found the following order for the acceleration of degradation: $BrO_3^- > H_2O_2 > S_2O_8^{2-}$. Yu et al. [3] have found that persulfate (0.1 mM) accelerates the degradation for reactive black 5 at pH 7. Gratzel et al. [10] and Pelizzeti et al. [11] have noticed the same positive effect for chlorophenol, 2,7 polychlorinated dibenzo dioxin, atrazine and organophosphorus compounds.

In all the cases, persulfate can be activated by different processes, including electron transfer Eq. (1), photolysis/heat Eq. (2), and the presence of metals Eq. (3) [12–14].

$$S_2O_8^{2-} + e^- \rightarrow SO_4^{\bullet-} + SO_4^{2-} \quad (1)$$

$$S_2O_8^{2-} + UV/heat \rightarrow SO_4^{\bullet-} + SO_4^{\bullet-} \quad (2)$$

$$S_2O_8^{2-} + M^{n+} \rightarrow SO_4^{\bullet-} + SO_4^{2-} + M^{n+1} \quad (3)$$

Activation of persulfate results in the formation of the sulfate radical ($SO_4^{\bullet-}$) under a broad range of pH ($1 \leq pH \leq 10.5$) [15].

The sulfate radical has a wide range of optical absorption (300 à 570 nm), with a maximum at 450 nm ($\varepsilon = 1100\ L\ s\ mol^{-1}\ cm^{-1}$) and is a strong oxidant, with a redox potential comprised between 2.6 and 3.1 V, relative to the normal hydrogen electrode (NHE) [16]. The sulfate radical reacts by three different ways: electron transfer, addition (on double bond or aromatic rings) or hydrogen abstraction [14,17,18]. In addition, the decarboxylation of most aliphatic acids can be efficiently achieved with $SO_4^{\bullet-}$ which is not the case with $OH^\bullet$ [19,20]. Furthermore, $SO_4^{\bullet-}$ oxidizes chloride ions in solutions near neutrality, being advantageous for the production of $Cl_2^{\bullet-}$, which is difficult to achieve with hydroxyl radicals [21].

Degradation studies of the UV/TiO_2/$K_2S_2O_8$ system have shown that they were dependent on the nature of the contaminant, the nature of the catalyst, the pH and the dosage of the oxidant [3–7]. However these studies were only limited to the effect of these factors on the degradation and no optimization was reported.

So it would be interesting to optimize the operational conditions for its use during the degradation by means of a chemometric approach based upon a surface response modeling. Response surface methodology (RSM) has been applied to model and optimize different wastewater treatment processes including adsorption [22], Fenton's oxidation [23], electrochemical oxidation [24], electrocoagulation [25] and photocatalytic degradation processes [26–28]. To accomplish this aim, imazalil, a fungicide from the family of imidazole, cited as carcinogen by the US.EPA, was used as a target for this optimization since its degradation, the identification of nine of its photoproducts and the reaction pathway were performed before. It was demonstrated that photocatalysis was responsible for its degradation while photochemistry only degraded 3% [29].

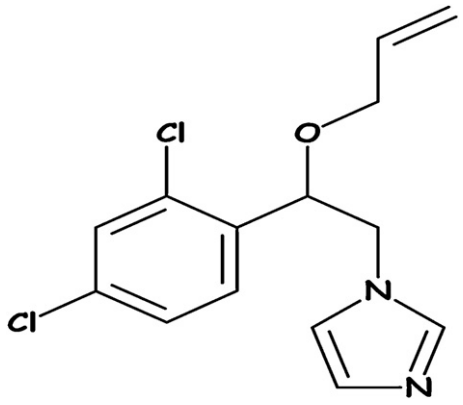

Fig. 1. Stucture of imazalil.

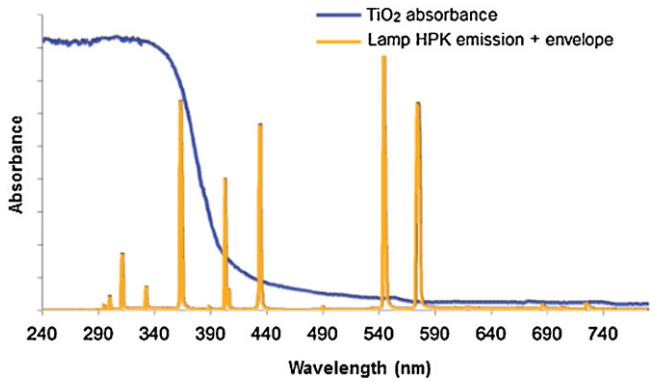

Fig. 2. Emission spectra of the HPK lamp and absorption spectra of TiO_2.

To the best of our knowledge, the optimization of the degradation of imazalil or any other molecule in the UV/TiO_2/$K_2S_2O_8$, using chemometric approach has never been reported.

So, the aim of this paper was to optimize the degradation of imazalil (see structure, Fig. 1) by the UV/TiO_2/$K_2S_2O_8$ system using a response surface methodology based on the central composite design. Important parameters, such as pH values, TiO_2 loading, imazalil concentration, and persulfate concentration were investigated in this study as well as the interactions between these different parameters. Furthermore, experiments with *tert*-butanol, a hydroxyl radical scavenger, were performed to figure out which radicals are predominant in the range of pH studied.

2. Materials and methods

2.1. Chemicals

Imazalil, (*RS*)-1-[2-(allyloxy)-2-(2,4-dichlorophenyl)ethyl]-1H-imidazole (99% purity) was purchased from Sigma–Aldrich and used as received. Titanium dioxide Degussa P25 was provided by Degussa (Frankfurt, Germany) with a specific BET area of 50 $m^2\,g^{-1}$ and a mean particle size of 30 nm. Polyvinylidene fluoride PVDF filters (0.45 μm) were purchased from Millipore. Acetonitrile (quality HPLC grade) and potassium persulfate ($K_2S_2O_8$) were purchased from Aldrich. Water was obtained from a Millipore Waters Milli-Q water purification system. Other reagents were at least of analytical grade.

2.2. Photoreactor and light source

The irradiation was carried out in an open borosilicate (Pyrex) glass cell (cut-off at 295 nm, 4 cm diameter, 9 cm height) equipped with a magnetic stirring bar and water circulating jacket. The light source was a HPK 125 W Philips mercury lamp with main emission wavelength at 365 nm, cooled with a water circulation. Fig. 2 shows the lamp emission spectra as well as TiO_2 absorption spectra. The radiant flux entering the irradiation cell was measured by a VLX-3 W radiometer with a CX-365 detector (UV-A). A value of 31 mW cm^{-2} was found by measuring the light coming through the bottom of the reactor. For all experiences, before and during irradiation, the suspensions were magnetically stirred.

2.3. Photocatalytic degradation procedure

Solutions of imazalil (50 mg L^{-1}) were prepared using Millipore Milli-Q deionized water and stored at 4 °C in the dark. For degradation experiments, the solutions were diluted from the stock solution into desired concentrations (25, 37.5, 50 mg L^{-1}) and irradiated. The pH values (3, 6.5 or 10) were adjusted by adding concentrated aqueous solutions of H_3PO_4 or NaOH to the desired value throughout the experiments. A magnetic stirrer was used to induce satisfactory mixing of the solution in the reactor. A volume of 25 mL of aqueous imazalil solution was introduced into the reactor and the required amount of TiO_2 (0.5, 1.5 or 2.5 g L^{-1}) powder and $K_2S_2O_8$ (0, 3 or 6 g L^{-1} equivalent to 0, 10 or 20 mM) were added according to the experimental design. Before irradiation, the suspension was stirred in the dark for 30 min to reach adsorption–desorption equilibrium.

When *tert*-butanol was used as a hydroxyl scavengers ([*tert*-butanol]/[imazalil] = 500), the same procedures were carried out using 25 mg L^{-1} of imazalil, 2.5 g L^{-1} of TiO_2 and 2.2 g L^{-1} of persulfate at the three different pH (3, 6.5 and 10).

2.4. Chemical analysis

Samples for analyses were withdrawn at regular time intervals and filtered through 0.45 μm PVDF syringe filters to remove TiO_2 particles immediately before analysis. Total volume of the sample withdrawn was less than 10% (by volume) of the suspension (*i.e.* 2.5 mL).

2.4.1. HPLC/DAD

The concentration profile of imazalil during irradiation was monitored using Shimadzu VP series HPLC system consisting of LC-10AT binary pump, a SPD-M10A DAD and Schimadzu Class-VP software version (5.0). A 20 μL of filtered irradiated samples were directly injected. Analytical separation was performed using a column KROMASIL C4 (250 mm × 4.6 mm, particle size 5 μm), mobile phase, 70:30 (v/v) acetonitrile/water and flow rate of 1 mL min^{-1}. The detection wavelength was 202 nm corresponding to the maximal wavelength of absorption for imazalil.

3. Experimental design data analysis

The chemometric approach was performed using a central composite design (CCD). Analysis of the experimental data was supported by the statistical graphics software system design expert 8.0.7.1 and stat graphics centurion XVI.

3.1. Experimental design

3.1.1. Choosing factors and response

It has been demonstrated by several authors that catalyst dosage, initial concentration of the target compound, UV light intensity, oxygen concentration, temperature, and pH for aqueous phase photoreactions were the main parameters affecting the degradation rate in the UV/TiO_2 system [26,28]. In this study, the concentration of persulfate was added. However, it is quite difficult to carry out an experimental design including all these factors because of the large number of experiments and complex data analysis required. Therefore, the most important factors were chosen from preliminary experiments in which the four following factors namely pH, TiO_2 loading, [imazalil], [persulfate] were retained. This means that all the experiments were carried out at constant temperature (20 °C), at constant photonic flux (31 mW cm^{-2}) and constant O_2 concentration (9 mg L^{-1}) in the central composite design.

An irradiation time corresponding to 90% imazalil photocatalytic degradation was chosen for the response factor. This variable was selected for two reasons: the first one is its fundamental and application importance, as one of the main goals of the photocatalytic treatment is the removal of the initial toxic substrate as fast as possible. One can say that the apparent kinetic rate constant k_{app} could be an alternative way nevertheless it is not an experimental measured value but a calculated one using a specific kinetic model

Table 1
Range of variation of the parameters used in the central composite design.

Variable	Symbol	Coded levels		
		Low (−1)	Center (0)	High (+1)
pH	A	3	6.5	10
TiO_2 ($g\,L^{-1}$)	B	0.5	1.5	2.5
[imazalil] ($mg\,L^{-1}$)	C	25	37.5	50
$[K_2S_2O_8]$ ($g\,L^{-1}$)	D	0	3	6

(*e.g.* first order kinetic) which might change with the experimental conditions and hence could induce a greater error. The second reason is that the removal time is not strongly related to the formation of reaction intermediates comparing to other variables used in previous recent studies such as decolorization efficiency (%) or TOC removal [26].

3.1.2. Central composite design

A response surface methodology based on the central composite design was used to determine the optimum conditions for photocatalytic degradation of imazalil by mixing TiO_2 and persulfate. Using codified values of the variables, such as pH, TiO_2 loading, imazalil concentration and persulfate concentration, it is possible to obtain a polynomial expression that semi-empirically describes the response. Table 1 summarizes the three levels for each factor involved in the design. These levels were chosen according to previous experiments carried out at our laboratory and also from data in the literature for similar laboratory experiments [5,6,30,31]. The central composite design consisted of 28 experiments divided into three blocks: (a) full factorial design 2^4 (16 experiments) corresponding to four variables ($n = 4$) at two levels: low (−1) and high (+1); (b) 8 ($2n$) axial points located at the center and both extreme levels; (c) 4 central replicates of the central points. Experiments were undertaken in random order to provide protection against the effects of lurking variables. Table 2 shows the CCF design matrix applied and the actual experimental results (*Y*exp) and data obtained from the center composite design (*Y*calc) for the response (*Y*) corresponding to removal time of 90% of imazalil. A semi-empirical expression in Eq. (4) consisting of 18 statistically significant coefficients was obtained from the data analysis using the statistical graphics software expert design at 95% confidence level ($p < 0.05$). This model explains perfectly the results in the experimental range studied (R^2 adjusted = 0.9915). Also, this can be seen by comparing the measured values against the predicted responses by the model for the removal time (Table 2). In addition, the coefficient of variation is less than 10% (CV = 5.9%). The model adequacy and significance was further evaluated by ANOVA (Analysis of Variance). The model *F*-value of 175.14 and its *p*-value less than 0.0001 implies the high significance of the model. This means that there is only a 0.01% chance that a "Model *F*-Value" could occur due to noise. So this confirms a good predictability of the model.

$$Y(\text{min}) = 19.68 + 14.00A - 5.17B + 10.22C - 10.25D + 1.63AB + 2.38AC + 4.13AD - 0.87BC + 3.63BD - 3.87CD + 3.29A^2 + 2.29C^2 + 3.54D^2 - 1.56ABD + 0.94ACD + 1.06BCD - 11.56AD^2 - 2.94C^2D \quad (4)$$

where A = pH, B = TiO_2, C = [Imazalil] and D = $[K_2S_2O_8]$.

In equation the sign (+) indicates that degradation time increases in the presence of high levels of the respective variables, meaning a negative effect from the photocatalytic point of view, while the sign (−) indicates that degradation time decreases in the presence of high levels, meaning a positive effect from the photocatalytic point of view. Positive quadratic or third order polynomial coefficients indicate a synergistic effect, while negative coefficients, an antagonistic effect between or among the variables.

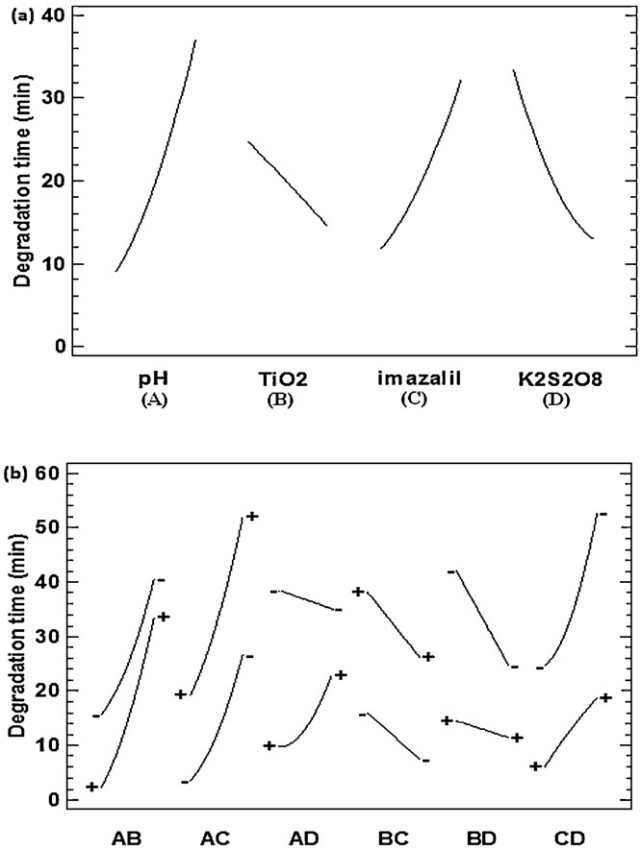

Fig. 3. Graphical presentation of the statistical evaluation of the individual factrors (a) and interactions of two factors (b) on the 90% of removal time of imazalil.

The importance of each individual factor as well as interactions depends on the coefficient in Eq. (4). For example it can be seen that persulfate ions play an important role when associated with other factors such as AD, CD and BD. Other interactions take place including AC, AB and BC as well as quadratic terms which are AA, CC and DD. Third order polynomial factors (BCD, ACD, CCD and ABD) are also present but in a lesser extent, except for ADD, but their significance is more difficult to interpret.

3.2. Screening of main effects

The influence of all the single factors (Fig. 3a) and interaction between them (Fig. 3b) are considered and the lines indicate the estimated change of response (time of 90% of degradation) as each factor is moved from its low to its high level.

3.2.1. Single factors

Fig. 3a shows the influence of single factors while maintaining all other factors constant at midway value codified as value 0, between their low and high values. The curve slope is proportional to the effect size whereas the line direction specifies a positive or negative influence of the effect.

3.2.1.1. pH value. The pH plays an important role among these factors according to its coefficient in Eq.(4). In the wide range 3–10, pH markedly influences the efficiency of the photocatalytic degradation of imazalil. As the pH increases, the time of degradation increases too. This result suggests that in presence of persulfate

Table 2
Experimental data in central composite design.

Experiment number	Variable levels (codified values)				Y_{exp} (min)	Y_{calc} (min)
	pH	C_{TiO_2} (g L^{-1})	$C_{imazalil}$ (mg L^{-1})	$C_{K_2S_2O_8}$ (g L^{-1})		
1	3 (−1)	0.5 (−1)	25 (−1)	0 (−1)	41.5	41.1
2	10 (+1)	0.5 (−1)	25 (−1)	0 (−1)	28.5	28.4
3	3 (−1)	2.5 (+1)	25 (−1)	0 (−1)	21.0	21.0
4	10 (+1)	2.5 (+1)	25 (−1)	0 (−1)	21.5	21.1
5	3 (−1)	0.5 (−1)	50 (+1)	0 (−1)	70.0	70.3
6	10 (+1)	0.5 (−1)	50 (+1)	0 (−1)	63.5	63.4
7	3 (−1)	2.5 (+1)	50 (+1)	0 (−1)	42.5	42.4
8	10 (+1)	2.5 (+1)	50 (+1)	0 (−1)	48.0	48.3
9	3 (−1)	0.5 (−1)	25 (−1)	6 (+1)	7.5	7.8
10	10 (+1)	0.5 (−1)	25 (−1)	6 (+1)	15.0	14.2
11	3 (−1)	2.5 (+1)	25 (−1)	6 (+1)	5.0	4.3
12	10 (+1)	2.5 (+1)	25 (−1)	6 (+1)	10.5	10.9
13	3 (−1)	0.5 (−1)	50 (+1)	6 (+1)	14.0	13.5
14	10 (+1)	0.5 (−1)	50 (+1)	6 (+1)	32.5	33.1
15	3 (−1)	2.5 (+1)	50 (+1)	6 (+1)	10.0	10.7
16	10 (+1)	2.5 (+1)	50 (+1)	6 (+1)	31.0	30.6
17	3 (−1)	1.5 (0)	37.5 (0)	3 (0)	8.5	9.0
18	10 (+1)	1.5 (0)	37.5 (0)	3 (0)	36.5	36.9
19	6.5 (0)	0.5 (−1)	37.5 (0)	3 (0)	23.0	24.8
20	6.5 (0)	2.5 (+1)	37.5 (0)	3 (0)	13.0	14.5
21	6.5 (0)	1.5 (0)	25 (−1)	3 (0)	10.0	11.7
22	6.5 (0)	1.5 (0)	50 (+1)	3 (0)	33.0	32.2
23	6.5 (0)	1.5 (0)	37.5 (0)	0 (−1)	33.0	33.4
24	6.5 (0)	1.5 (0)	37.5 (0)	6 (+1)	12.5	12.9
25	6.5 (0)	1.5 (0)	37.5 (0)	3 (0)	21.0	19.7
26	6.5 (0)	1.5 (0)	37.5 (0)	3 (0)	21.0	19.7
27	6.5 (0)	1.5 (0)	37.5 (0)	3 (0)	21.0	19.7
28	6.5 (0)	1.5 (0)	37.5 (0)	3 (0)	21.0	19.7

working in acidic conditions is better for the degradation of imazalil.

The interpretation of pH effect as it was shown by other authors [26,31] can be explained by taking into account different points.

For pH values lower than the pHpzc of titania (pH 6.25), the surface becomes positively charged whereas for pH values higher than pHpzc, the surface becomes negatively charged according to the following equilibrium:

$$pH < pH_{pzc}: \quad Ti{-}OH + H^+ \rightarrow TiOH_2^+ \tag{5}$$

$$pH > pH_{pzc}: \quad Ti{-}OH + OH^- \rightarrow TiO^- + H_2O \tag{6}$$

Since the pKa of imazalil is 6.53 [32], its adsorption at pH < pH_{pzc} on the TiO_2 surface should decrease due to the positive charges present both on imazalil and TiO_2 surface and so by taking into account the Langmuir–Hinshelwood (L–H) model (by assuming that the kinetic results follow this model), a decrease in the rate of the degradation can be expected as it was found in previous results [29]. In addition, it is known that at alkaline pH, the rate of $OH^\bullet$ is higher than at acidic pH. As in the UV/TiO_2/$K_2S_2O_8$ system the observed reactivity is the highest at acidic pH, we can hypothesize that the presence of persulfate is mainly responsible of this behavior.

Otherwise, Liang and Su [33] studied the inter-conversion from sulfate radical to hydroxyl radical by the following reaction Eq. (7):

$$SO_4^{\bullet-} + OH^- \rightarrow SO_4^{2-} + OH^\bullet \quad k = 1.4 \times 10^7 \text{to} 7.3 \times 10^7\ M^{-1}\ s^{-1} \tag{7}$$

and they observed that:

At pH < 7: $SO_4^{\bullet-}$ is the predominant radical.

At pH = 9: $OH^\bullet$ and $SO_4^{\bullet-}$ are both present.

At pH > 9: $OH^\bullet$ is the predominant radical.

At acidic pH, both $S_2O_8^{2-}$ and $HS_2O_8^-$ can be found according to the following reaction [34]:

$$S_2O_8^{2-} + H^+ \leftrightarrows HS_2O_8^- \quad K < 0.05 \tag{8}$$

Then, these both species can react easily on the surface of TiO_2 (positively charged) with electron photogenerated in the conduction band to lead to the formation of the reactive $SO_4^{\bullet-}$ species and prevent the recombination between electron and hole.

In this context we might conclude that at acidic pH, persulfate is an efficient electron scavenger and that sulfate radicals are powerful oxidants.

3.2.1.2. TiO_2 loading. TiO_2 loading has a positive influence on the degradation ((−) sign in Eq. (4)). Generally, photocatalytic rate increases with TiO_2 loading increasing due to higher surface area of TiO_2 that is beneficial to adsorption and degradation. From Fig. 3a it can be seen that as the amount of TiO_2 increases, the photocatalytic efficiency increases proportionally.

3.2.1.3. Imazalil concentration. The variation of removal time is approximately linear with respect to the concentrations studied (Fig. 3a), as the concentration of imazalil increases, the removal time increases too. An increase in the fungicide concentration leads to an increase in the initial rate of degradation according to L–H model, but also in the removal time since further molecules to be degraded are present in solution.

3.2.1.4. Persulfate concentration. Persulfate plays an important role in the photocatalytic system, since an increase in its concentration leads to a decrease in the removal time (Fig. 3a). An increase in the concentration of persulfate means that further sulfate radicals will be generated by photolysis, thermal activation or from the electron in the conduction band.

3.2.2. Quadratic interactions

The quadratic terms, indicate which way the response surface is bending (the curvature of the surface). The sign of the term is positive when the surface is convex and negative when the surface is concave. In our results, positive quadratic interactions occurs for three parameters (DD > AA > CC, Eq. (4)) corresponding to convex surfaces (Fig. 3a) and showing a higher time of degradation at lower pH and concentration of imazalil and at higher persulfate

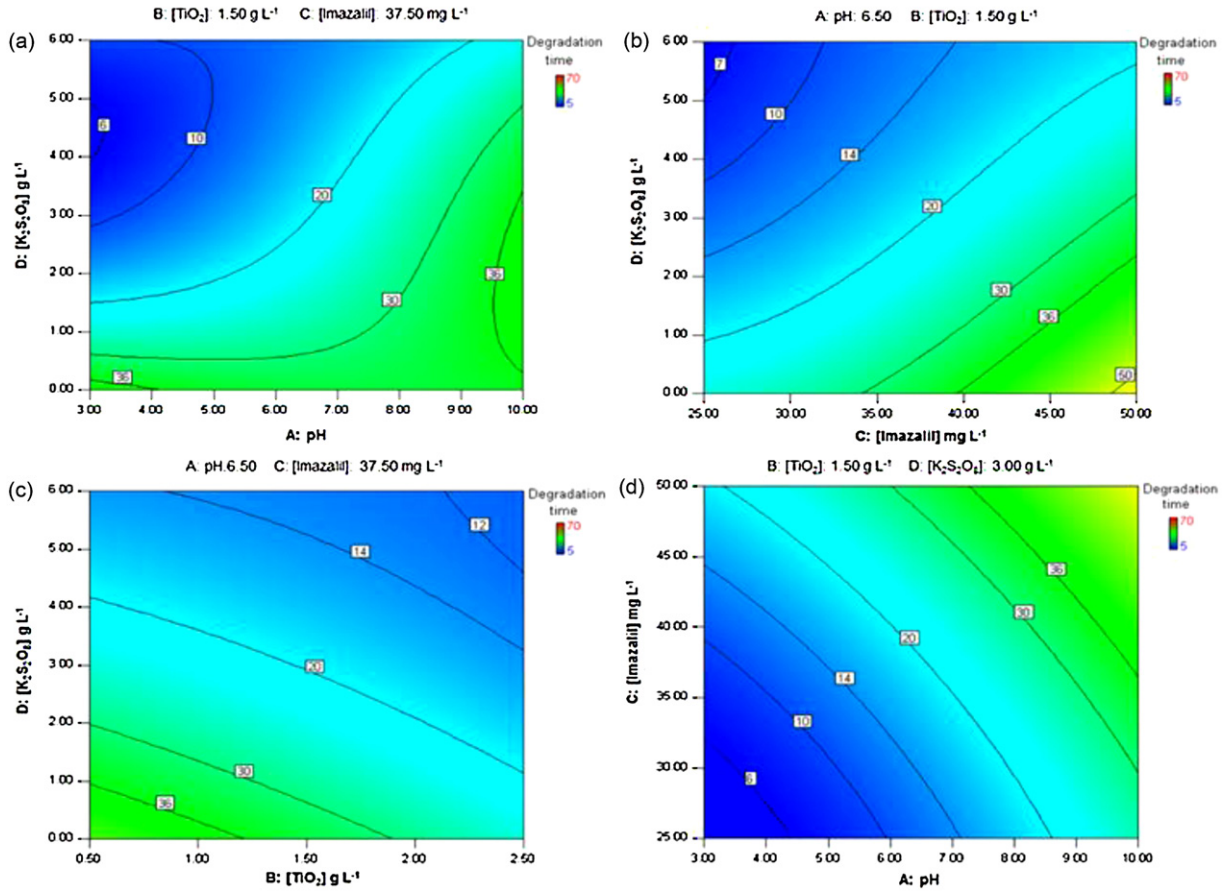

Fig. 4. Contour plots of the 90% of removal time of imazalil for the four most important pair of factors.

concentration. For example while an increase of persulfate concentration causes a decrease of the degradation time; a too high persulfate concentration causes an increase of the degradation time. Such a result could be explained by the fact that an excess of persulfate concentration produces a lot of sulfate anions Eq. (1) [35] which can compete for the adsorption on TiO_2 surface or react with reactive radicals according to the following equation (Eq. (9)).

$$SO_4^{2-} + OH^{\bullet} \rightarrow SO_4^{\bullet -} + OH^- \quad (9)$$

Fortunately, in our experimental conditions, all these positive quadratic interactions do not exhibit a significant influence on the degradation. It is noteworthy that TiO_2/TiO_2 (BB) is not present in Eq. (4) leading to the conclusion that scattering effect of TiO_2 does not occur and that we are still in the optimal range.

3.2.3. *Interactions between the different parameters*

Fig. 3b should allow us to better understand the meaning of the interactions between factors. An interaction between variables occurs when the change in response from the low level to the high level of one variable is not the same as the change in response at the same two levels of a second variable. That is, the effect of one variable is dependent upon a second variable. Any discrepancy between the two lines (lines marked with + and −) can be attributed to a significant interaction between the factors in question.

From Fig. 3b we can see that the most important interactions were pH/[$K_2S_2O_8$] (AD), [Imazalil]/[$K_2S_2O_8$] (CD), TiO_2/[$K_2S_2O_8$], (BD), pH/[$K_2S_2O_8$] (AC) and pH/[Imazalil] (AB) but the most relevant were AD and CD.

Considering pH/[$K_2S_2O_8$] interaction (AD), Fig. 3b shows that significant interactions take place. In the absence of persulfate, the degradation time decreases as the pH increases, because at alkaline pH, the adsorption of imazalil is higher and also more hydroxyl radicals are produced. For the highest concentration of persulfate and at acidic pH, the removal time was low due to the presence of a high quantity of persulfate which can be adsorbed on TiO_2 surface to avoid e^-/h^+ recombination and able to generate sulfate radicals.

Coming to the interaction between imazalil and persulfate (CD), we can see that whatever the $K_2S_2O_8$ concentration, an increase in imazalil concentration leads to an increase in the time of degradation as expected.

For TiO_2/[$K_2S_2O_8$] interaction (BD), plots indicate that without persulfate, the degradation time is strongly correlated with the amount of TiO_2 (when the quantity of TiO_2 increases, the time of degradation decreases) but when persulfate is added, the degradation time decreases and the persulfate concentration becomes the determining factor for the degradation time.

On the other hand, less significant interactions were observed between pH and imazalil concentration (AC) as well as between pH and TiO_2 (AB). Whatever the imazalil concentration or the TiO_2 loading, a faster removal occurred at acidic pH (Fig. 3b).

These findings show that interactions between almost all these factors can be found. Such information would not be acquired in a univariate study (one factor at a time) of the photocatalytic process and thus, the use of experimental design of experiments over the conventional univariate optimization is necessary.

3.3. *Response surface plots and optimization conditions*

After performing a screening of factors and their interactions, the response surface analysis was carried out, in order to find the

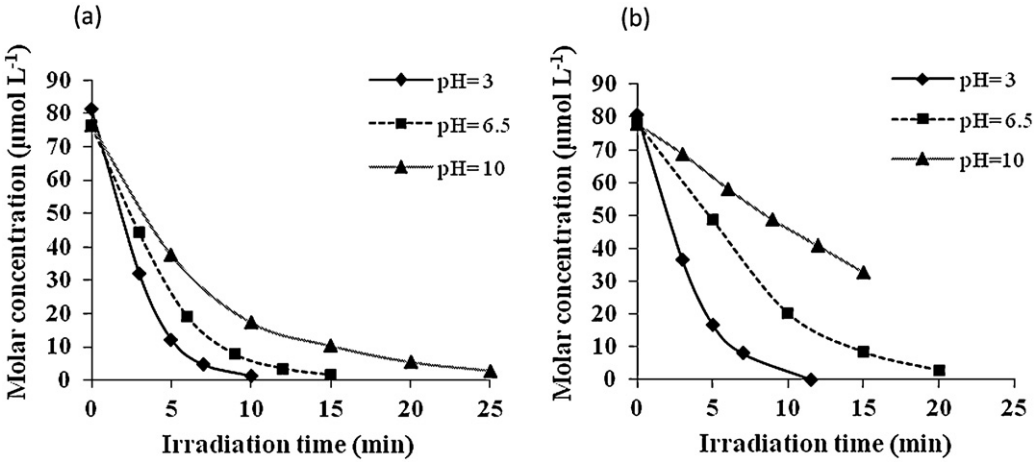

Fig. 5. Degradation of imazalil (84.1 μM) in the system UV/TiO_2/$K_2S_2O_8$ without *tert*-butanol (a) and with *tert*-butanol (b).

optimal conditions for the degradation of imazalil in the range studied.

Response surface plots provides a method to predict the time necessary to achieve a 90% disappearance of imazalil (removal time) for different values of the test variables.

In addition, the contours of the plots help in the identification of the type of interactions between the selected variables [36]. Each contour curve represents an infinite number of combinations of the two selected variables with the other maintained at their respective zero coded level. A circular contour of response surfaces indicates that the interaction between the corresponding variables is negligible. An elliptical or saddle nature of the contour plots indicates that the interaction between the corresponding variables is significant [26]. Also the use of the three dimensional response surfaces gives clearer insight for the interactions occurring (supplementary informations).

In Fig. 4, are displayed the contour plots of the removal time for the four most important pairs of factors: pH *versus* persulfate concentration, AD (Fig. 4a), initial concentration of imazalil *versus* persulfate concentration, CD (Fig. 4b), TiO_2 concentration *versus* persulfate concentration, BD (Fig. 4c) and pH *versus* initial concentration of imazalil, AC (Fig. 4d).

The optimal conditions for the fastest removal of imazalil were obtained from the figures below:

Fig. 4a exhibits the contour plots for pH *versus* persulfate concentration (TiO_2 1.5 g L^{-1} and [Imazalil] = 37.5 mg L^{-1}). The saddle nature of the contour plots confirms that a significant interaction exists between these two factors. The most suitable conditions to have a removal time of about 6 min are low pH values (3–3.5) and persulfate concentration comprised between 4 and 5 g L^{-1}. A persulfate concentration higher than 5 g L^{-1} does not allow obtaining a better efficiency.

Fig. 4b shows the contour plots of imazalil concentration *versus* persulfate concentration (TiO_2 = 1.5 g L^{-1} and pH = 6.5). A fast removal time (<7 min) can be achieved for concentrations of imazalil around 25–27 mg L^{-1} and persulfate concentration comprised between 5 and 6 g L^{-1}. This indicates that persulfate and imazalil concentration critically affect the rate of the pesticide degradation but the interaction between them is not very remarkable since contour plots are almost circular.

Fig. 4c represents the contour plots for TiO_2 loading *versus* persulfate concentration (pH = 6.5 and [imazalil] = 37.5 mg L^{-1}). The fastest removal time (12 min) is obtained with a TiO_2 concentration >2 g L^{-1} and a persulfate concentration comprised between 4.5 and 6 g L^{-1}.

Fig. 4d represents the contour plots for pH *versus* imazalil concentration (TiO_2 = 1.5 g L^{-1} and persulfate concentration = 3 g L^{-1}). To obtain removal time less than 7 min, pH < 5 and imazalil concentration < 35 mg L^{-1} are required.

3.4. Model validation and confirmation

Validation experiments were carried out at the optimal conditions for TiO_2 loading derived from multivariate design, as shown in Table 3. pH, was set at a value close to pH of neutral water (pH = 6.5), imazalil was chosen at an arbitrary value of 25 mg L^{-1} and persulfate concentrations were varied from 2.4 to 6 g L^{-1}. Results show that the experimental values are relatively close to the predicted values from semi-empirical expression Eq. (4), which confirms the adequacy and validity of the model simulating the removal time of imazalil.

3.5. Dominant radicals during the degradation

In order to better understand which radicals (hydroxyl or sulfate radicals) are involved during the degradation for the different pH studied in the experimental design, experiments using *tert*-butanol were performed. This latter is a scavenger for both hydroxyl and sulfate radicals but with different kinetic rate constants for both radicals: $kOH^{\bullet} = 6 \times 10^8\ M^{-1}\ s^{-1}$ and $kSO_4^{\bullet -} = 8 \times 10^5\ M^{-1}\ s^{-1}$ [37]. From a previous work [29] in which methanol and isopropanol were used as hydroxyl scavengers for the photocatalytic degradation of

Table 3
Comparison of predicted and experimental values of the response at optimal region for TiO_2 loading and imazalil concentration for another two experiments.

pH	C_{TiO_2} (g L^{-1})	$C_{imazalil}$ (mg L^{-1})	$C_{K_2S_2O_8}$ (g L^{-1})	Time for 90% degradation (min)		
				Predicted[a]	Observed[b]	Experimental error
6.5	2.5	25	2.4	9.0	9.5	5%
6.5	2.5	25	6	4.3	6.0	33%

[a] The values were calculated from semi-empirical expression (Eq.(4)).
[b] Average value on 90% degradation time of two experiments at selected condition.

imazalil, it was shown that a ratio of [alcohol]/[imazalil] = 500 was sufficient to inhibit the majority of hydroxyl radicals. Here a ratio of $[K_2S_2O_8]$/[imazalil] = 100 was selected to avoid as much as possible interference between *tert*-butanol and $SO_4^{\bullet -}$.

Fig. 5 shows the results obtained for the degradation of imazalil (25 mg L^{-1}) without (Fig. 5a) and with *tert*-butanol (Fig. 5b) for the system UV/TiO_2/$K_2S_2O_8$. We can see different percent of inhibition of degradation according to the pH studied. At pH = 3, the influence of *tert*-butanol remains low (only 7% of inhibition), while an increase of the pH provokes an increase of the inhibition, which goes from 33 to 52% for pH comprised between 6.5 and 10. So it can be concluded that at acidic pH, sulfate radicals are the main reactive species in solution, and if the pH increases the role played by hydroxyl radicals becomes more and more important [33].

These results confirm that at acidic pH, $S_2O_8^{2-}$ is well adsorbed at the TiO_2 surface and that $SO_4^{\bullet -}$ radicals formed are mainly responsible of the imazalil degradation.

4. Conclusions

The degradation of imazalil using an experimental design methodology was studied. The pH, TiO_2 loading, imazalil concentration and persulfate concentration were systematically evaluated *via* the center composite design based on response surface methodology. A semi-empirical expression was proposed and successfully used to model the photocatalytic process with a high correlation, and an optimal experimental region was also obtained through the contour diagram plots. In order to have faster removal time for the degradation of 25 mg L^{-1} of imazalil, acidic pH (3–4), persulfate concentration around 2.5 g L^{-1} and a TiO_2 loading of 2.5 g L^{-1} were required. This should be of great importance for the optimization of the experimental conditions for technological and industrial applications because we obtain the maximum of efficiency with the minimum amount of consumers. Further experiments on other compounds with different chemical structures will help prove, or disprove, the general applicability of this approach for optimization of UV/TiO_2/$K_2S_2O_8$ processes. On the other hand, experiments performed at acidic pH with *tert*-butanol showed that sulfate radicals are the major radicals involved in the degradation but if the pH increases the role played by hydroxyl radicals becomes more important.

Acknowledgement

The authors are thankful to the Region Rhone-Alpes for financing a part of this work in the frame of C-Mira project.

Appendix A. Supplementary data

Supplementary data associated with this article can be found, in the online version, at http://dx.doi.org/10.1016/j.apcatb.2012.12.021.

References

[1] A. Huber, M. Bach, H.G. Frede, Agriculture, Ecosystems and Environment 80 (2000) 191–204.
[2] I.K. Konstantinou, T.A. Albanis, Applied Catalysis B: Environmental 49 (2004) 1–14.
[3] C.-H. Yu, C.-H. Wu, T.-H. Ho, P.K. Andy Hong, Chemical Engineering Journal 158 (2010) 578–583.
[4] K. Selvam, M. Muruganandham, I. Muthuvel, M. Swaminathan, Chemical Engineering Journal 128 (2007) 51–57.
[5] A. Syoufian, K. Nakashima, Journal of Colloid and Interface Science 317 (2008) 507–512.
[6] N. Kashif, F. Ouyang, Journal of Environmental Sciences 21 (2009) 527–533.
[7] L. Ravichandran, K. Selvam, M. Swaminathan, Separation and Purification Technology 56 (2007) 192–198.
[8] A. Tsitonaki, B. Petri, M. Crimi, H. Mosbaek, R.L. Siegrist, P.L. Bjerg, Critical Reviews in Environmental Science and Technology 40 (2010) 55–91.
[9] A.R. Khataee, Polish Journal of Chemical Technology 11 (2009) 38–45.
[10] C.K. Gratzel, M. Jirousek, M. Gratzel, Journal of Molecular Catalysis 60 (1990) 375–387.
[11] E. Pelizzetti, C. Minero, V. Maurino, Advances in Colloid and Interface Science 32 (1990) 271–316.
[12] K.L. Ivanov, E.M. Glebov, V.F. Plyusnin, Y.V. Ivanov, V.P. Grivin, N.M. Bazhin, Journal of Photochemistry and Photobiology A: Chemistry 133 (2000) 99–104.
[13] L. Dogliotti, E. Hayon, Journal of Physical Chemistry 71 (1967) 2511–2516.
[14] P. Neta, V. Madhavan, H. Zemel, R. Fessenden, Journal of the American Chemical Society 99 (1977) 163–164.
[15] G.P. Anipsitakis, D.D. Dionysiou, Applied Catalysis B: Environmental 54 (2004) 155–163.
[16] M. Antoniou, A. de la Cruz, D. Dionysiou, Environmental Science and Technology 44 (2010) 7238–7244.
[17] O.P. Chawla, R.W. Fessenden, Journal of Physical Chemistry 79 (1975) 2693–2700.
[18] R.E. Huie, C.L. Clifton, Journal of Physical Chemistry 94 (1990) 8561–8567.
[19] V. Madhavan, H. Levanon, P. Neta, Radiation Research 76 (1978) 15–22.
[20] M.J. Davies, B.C. Gilbert, C.B. Thomas, J. Young, Journal of the Chemical Society, Perkin Transactions 1 2 (1985) 1199–1204.
[21] D. Wang, Y. Li, M. Yang, M. Han, Science of the Total Environment 393 (2008) 64–71.
[22] G. Annadurai, R.S. Juang, D.J. Lee, Advances in Environmental Research 6 (2002) 191–198.
[23] M. Ahmadi, F. Vahabzadeh, B. Bonakdarpour, E. Mofarrah, M. Mehranian, Journal of Hazardous Materials 123 (2005) 187–195.
[24] A. Gurses, M. Yalcin, C. Dogar, Waste Management 22 (2000) 491–494.
[25] T. Ölmez, Journal of Hazardous Materials 162 (2009) 1371–1378.
[26] M. Sleiman, D. Vildozo, C. Ferronato, J.-M. Chovelon, Applied Catalysis B: Environmental 77 (2007) 1–11.
[27] D. Vildozo, C. Ferronato, M. Sleiman, J.-M. Chovelon, Applied Catalysis B: Environmental 94 (2010) 303–310.
[28] Y. Lin, C. Ferronato, N. Deng, F. Wu, J.-M. Chovelon, Applied Catalysis B: Environmental 88 (2009) 32–41.
[29] R. Hazime, C. Ferronato, L. Fine, A. Salvador, F. Jaber, J.-M. Chovelon, Applied Catalysis B: Environmental 126 (2012) 90–99.
[30] E. Vulliet, J.M. Chovelon, C. Guillard, J.M. Herrmann, Journal of Photochemistry and Photobiology A: Chemistry 159 (2003) 71–79.
[31] I. Bouzaida, C. Ferronato, J.M. Chovelon, M.E. Rammah, J.M. Herrmann, Journal of Photochemistry and Photobiology A: Chemistry 168 (2004) 23–30.
[32] M.R. Siegel, A. Kerkenaar, A. Kaars Sijpesteijn, European Journal of Plant Pathology 83 (1977) 121–133.
[33] C. Liang, H.W. Su, Industrial and Engineering Chemistry Research 48 (2009) 5558–5562.
[34] S.S. Gupta, Y.K. Gupta, Inorganic Chemistry 20 (1981) 454–457.
[35] W. Liu, S. Chen, W. Zhao, S. Zhang, Desalination 249 (2009) 1288–1293.
[36] D.C. Montgomery, Design and Analysis of Experiments, 5th ed., John Wiley and Sons, New York, 2001.
[37] G.V. Buxton, C.L. Greenstock, W.P. Helman, A.B. Ross, Journal of Physical and Chemical Reference Data 17 (1988) 513–886.